

# Application of Fast Non-Local Denoising Approach in Digital Radiography Using Lung Nodule Phantom for Radiation Dose Reduction

Jina Shim<sup>1</sup>, Myonggeun Yoon<sup>2</sup>, Youngjin Lee<sup>3\*</sup>

1. Department of Diagnostic Radiology, Severance Hospital, Seoul, Republic of Korea
2. Department of Bio-Convergence Engineering, Korea University, Seoul, Republic of Korea
3. Department of Radiological Science, Gachon University, 191, Hambakmoero, Yeonsu-gu, Incheon, Republic of Korea

ARTICLE INFO	ABSTRACT
<b>Article type:</b> Original Paper	<b>Introduction:</b> Chest X-ray imaging has become the most commonly used, as it is the primary method for lung cancer screening during medical check-ups. The radiation dose should be minimized to ensure that the patients are not overexposed to radiation. However, radiation dose reduction results in increased noise in the chest X-ray image. Thus, the purpose of this study was to evaluate the utility of fast non-local means (FNLN) filters to reduce radiation dose while maintaining sufficient image quality.
<b>Article history:</b> Received: Aug 28, 2021 Accepted: Jan 25, 2022	<b>Material and Methods:</b> This study evaluates three filters (median, Wiener, and total variation) and a newly proposed filter (fast non-local means (FNLN)), which reduce image noise. A realistic anthropomorphic phantom is used to compare images acquired depending on positions such as anterior-posterior, lateral, and posterior-anterior, using a self-produced 3D printed lung nodule phantom. To evaluate image quality, we used the normalized noise power spectrum (NNPS), contrast to noise ratio (CNR), and coefficient of variation (COV) evaluation parameters.
<b>Keywords:</b> Digital Radiography X-Ray Image Denoising Fast Non-Local Means (FNLN) Approach 3D Printing Quantitative Evaluation of Image Quality	<b>Results:</b> The NNPS and COV were lowest and the CNR was highest with FNLN images. FNLN filter outperforms other compared filters in terms of noise reduction. <b>Conclusion:</b> Therefore, the use of an FNLN filter is recommended, because it reduces the radiation dose to a patient and thus minimizes the risk of cancer, while maintaining diagnostic quality.

► Please cite this article as:

Shim J, Yoon M, Lee Y. Application of Fast Non-Local Denoising Approach in Digital Radiography Using Lung Nodule Phantom for Radiation Dose Reduction. Iran J Med Phys 2022; 19: 363-370. 10.22038/IJMP.2022.60000.2009.

## Introduction

The use of diagnostic imaging has increased significantly over the years owing to numerous technological developments. Between 1980 and 2006, the medical exposure of the population in the United States increased by approximately 33% [1]. Korea is no exception; according to the International Commission on Radiological Protection (ICRP) report, the frequency of diagnostic radiologic examinations increased steadily from 2006 to 2011 [2]. In particular, the frequency of chest X-ray examinations performed in Korea has increased. Chest X-ray examination, which is the primary examination to detect lung nodules, has contributed significantly to the efficient diagnosis of diseases. The detection of malignant lung nodules can significantly help to prevent cancer. However, as the chest is anatomically complex, it is difficult to obtain high-quality radiological chest images. More specifically, structures such as lung, spine, and mediastinum are not easily recognized in radiographic images simultaneously as such structures with largely different contrast are in one location. Therefore, to lower the contrast, a high-

tube-voltage technique has been established, which improves the diagnostic quality of chest images [3]. However, these techniques result in an increased effective dose for the patient [4, 5].

Medical radiation can be beneficial to a patient. However, as ionization radiation damages deoxyribonucleic acid (DNA) directly, which can result in cancer, radiation exposure can induce harm if not used properly. In fact, there is a linear relationship between the likelihood of developing cancer and radiation dose, and the former increases even at low doses [6]. Increasing medical radiation exposure has raised concerns about the increased risk of cancer, which is also a public health issue at present that will continue in the future [7]. Therefore, in chest X-ray examinations, which are being performed not only on patients, but also on the general public, radiation exposure should be lowered while maintaining diagnosable image quality. One approach in the effort to minimize radiation exposure involves suppressing noise in images. Reducing the radiation dose may severely degrade the image, resulting in excessive

\*Corresponding Author: Tel: +82-10-4012-3081; Fax: 82-31-740-7264; Email: yj20@gachon.ac.kr

noise, specifically electronic and quantum noise. By eliminating the excess noise, high image quality can be maintained even at low doses [8, 9]. Conventional filters have been used to suppress noise. One is the median filter, which is a nonlinear method used to remove noise, particularly the salt-and-pepper type, while maintaining edge details. Another, called the Wiener filter, can be considered as one of the most fundamental noise reduction methods. The Wiener filter is a low-pass filtering method based on the least squares principle in the frequency domain, and has the advantage of more accurately analyzing the distribution of noise compared to the median filter [10]. In addition, the total variation (TV) filter restores a deteriorated image by reflecting a correlation to the overall image configuration variable for a certain region by setting a certain region around the pixel value of the region of interest. The TV minimization method using iterative reconstruction is one of the most widely used methods for image noise reduction [11, 12]. The TV filter uses an algorithm that minimizes the integral value of absolute gradients in an image. Because artifacts and noise usually represent high absolute gradients, TV filters can effectively reduce high-frequency elements, such as streak artifacts. However, with these filters, weak edges in particular are still damaged. To address this problem, fast non-local means (FNLM) filters, as proposed by J. Darbon et al. [13], have provided noticeable improvements. This filter is used to compute the similarity between two pixels by estimating the Euclidean distance between two image patches. It is suitable for preserving the edge of an image deteriorated by noise.

Studies on phantoms have been conducted before tests on patients to obtain the correlation between radiation dose and image quality. In particular, the commercial nodule phantom is a useful tool to obtain quantitative information about the correlation

between the detection probability of a nodule and image quality [14]. However, the commercial nodule phantom has shown a limitation in representing a malignant nodule. As the shape of some commercial nodule phantoms is consistent with a sphere, malignant nodules cannot be reliably represented.

This study quantitatively compares the performance of an FNLM filter with those of the median, Wiener, and TV filters. Chest phantom images, including self-produced 3D printed lung nodule phantoms, were acquired for each position (anterior-posterior (AP), lateral (LAT), and posterior-anterior (PA)) by reducing the radiation dose, while maintaining sufficient image quality.

## Materials and Methods

### Experimental Study

#### Lung nodule phantom produced using 3D printing

Figure 1 shows the process of nodule phantom fabrication. Four patients who were diagnosed with irregular-shaped and lobulated-shape nodules from a low-dose chest computed tomography (CT) scan were randomly selected. CT Digital Imaging and Communications in Medicine (DICOM) images of the selected patients were loaded in the TeraRecon 3D program (TeraRecon, San Mateo, CA, USA). Nodules were segmented while checking axial, coronal, and sagittal CT images. The segmented nodules were converted to STL file format with the smoothness of 100 and the decimate of 20, as recommended by the manufacturer. The created STL nodule files were converted to g-code, ready to be 3D printed. The 3D printer (RS pro 800 SLA stereo lithography apparatus, UnionTech, Illinois, USA) printed the lung nodule phantom using a stereolithography method, made of hardening liquid plastic materials by shooting a laser and the employed material, which was polylactic acid. The volumes of the fabricated nodule phantoms were 0.219, 0.649, 0.715, and 1.668 cm<sup>3</sup>.

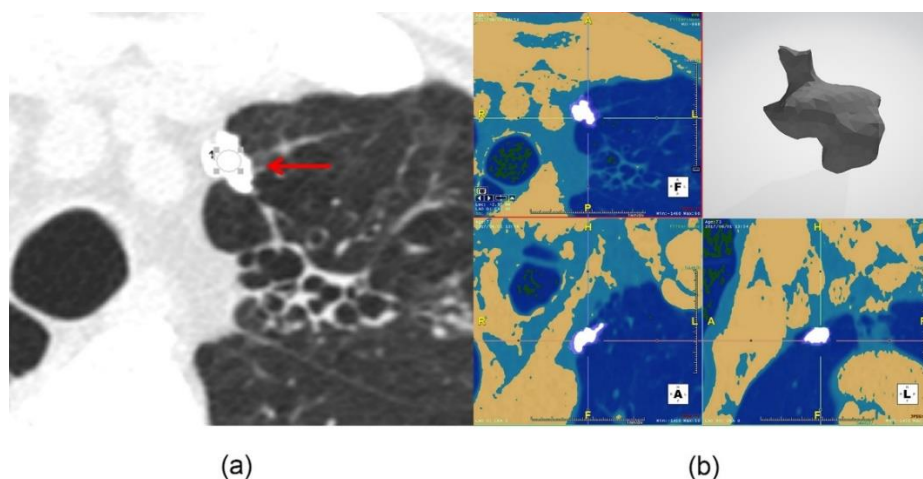


Figure 1. Nodule phantom fabricated using nodule segmentation in CT image: (a) 1.25-mm-thin slice CT axial image including segmentation area acquired for nodule phantom production and (b) phantom production process using TeraRecon software

**Technical parameters**

Figure 2 presents the experimental conditions and phantom structure. A multipurpose anthropomorphic male chest phantom (N1 “LUNGMAN”, Kyoto Kagaku Co., Ltd., Kyoto, Japan) was used. The image of the phantom was acquired at the AP, LAT, and PA positions. A pathology was simulated through the insertion of all four lung nodules. The lung nodules were positioned as follows: two on the right lung and two on the left lung. A digital radiography system (Innovision-SH, SHIMADZU, Japan) was used with an added filtration of 2.0-mm aluminum and source-to-image distance of 180 cm. In the AP and PA positions, the tube charge was gradually increased to 1, 2, 3.2, 4, and 5 mAs. The tube voltage was maintained at 120 kVp. Subsequently, the tube charge was fixed to 3.2 mAs, and the tube voltage was changed to 90, 100, and 110 kVp to acquire the phantom images. In the LAT position, the tube charge was gradually increased to the values of 2, 4, 5, 10, 20, and 30 mAs. Meanwhile, the tube voltage was maintained at 120 kVp. Finally, the tube charge was fixed to 5 mAs and the tube voltage was changed to 90, 100, and 110 kVp.

**Fast non-local means (FNLM)**

The FNLM filter was proposed by J. Darbon et al. [13] in the late 2000s and has been developed to efficiently compute large calculations, which was a drawback of the non-local means filter proposed by Buades et al. [12,15]. This filter removes noise by calculating weights based on the structural similarity of surrounding pixels and taking the average of the weights, which is similar to a Gaussian filter or a bidirectional filter. These conventional filters are different in that only pixel  $m$  and the adjacent pixels are weighted, while the FNLM filter calculates the distance  $L$  in patches to obtain a weight. A patch is a concept that represents a set of pixels in a square region around any pixel. The FNLM filter simply does not consider the difference between two pixel values when weighing a pixel. Instead, the FNLM filter calculates the weight between two pixels by calculating the difference through all  $S \times S$ -sized pixels in the patch, formed around pixels  $c$  and  $d$ . When weights are calculated, a high similarity of grayness in surrounding pixels results in high weight. New filters, which reduce image noise, are characterized

by the use of an entire image, unlike the existing local filters [15-18]. The FNLM filter algorithm is defined as below;

$$NL[I](c) = \sum_{d \in I} w(c, d)I(d), \tag{1}$$

where  $I(c)$  and  $I(d)$  represent the brightness at pixels  $c$  and  $d$ , respectively, and  $w(c, d)$  is a weight for each region that satisfies  $0 \leq w(c, d) \leq 1$  and  $\sum_{d \in I} w(c, d) = 1$ . The weight for each region can be expressed as below;

$$w(c, d) = \frac{1}{Z(c)} S_{\lambda}(I(c + P) - I(d - P)), \tag{2}$$

where  $P$  is the local patch size when the image is vectorized to 1D, and  $\lambda$  is  $d-c$  [13,17]. If the weight is calculated as above, the computation amount is determined independently of the size of the patch, and could be then calculated more efficiently compared with that required by the existing non-local means (NLM).

**Quantitative analysis of the images**

The quantitative evaluation of the images were conducted using normalized noise power spectrum (NNPS), coefficient of variation (COV), and contrast-to-noise ratio (CNR). As shown in Fig. 3, all images were evaluated in ROIs A and B. In Fig. 3, the pixel of ROI was  $136 \times 136$  pixels, and in the case of AP and PA positions, a quantitative evaluation was performed on the inside of the heart, which is a noisy space due to the thick effective thickness in the chest, and in the case of LAT, a quantitative evaluation was conducted on the costophrenic (CP) angles, where sharpness is the most important anatomically. The NNPS is the noise value in the image, which depends on the frequency, allowing measurement of the image noise, which varies depending on the amount of radiation [20]. The COV is known as the relative error. A smaller COV value implies that images are corrupted with a small amount of noise [21]. The CNR is a parameter for evaluating an image by analyzing the contrast characteristic through the signal of the selected ROI and the background noise [22].

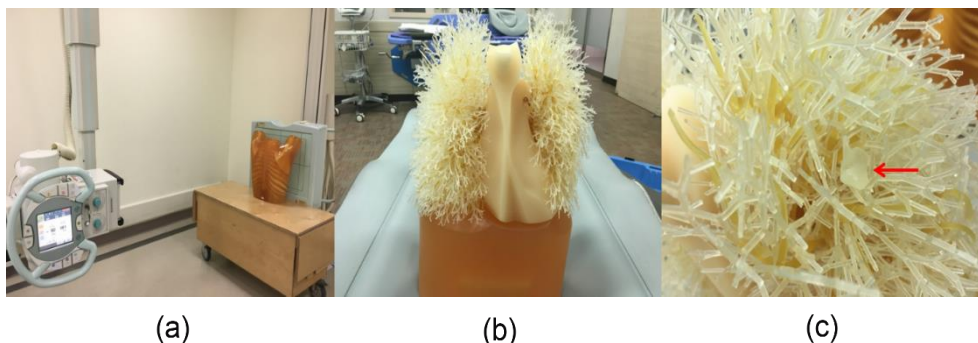


Figure 2. (a) Photograph showing experimental setup, including X-ray tube, detector, and chest phantom. (b) The inner appearance of the LUNGMAN phantom. (c) magnified image of nodule phantom located inside LUNGMAN phantom

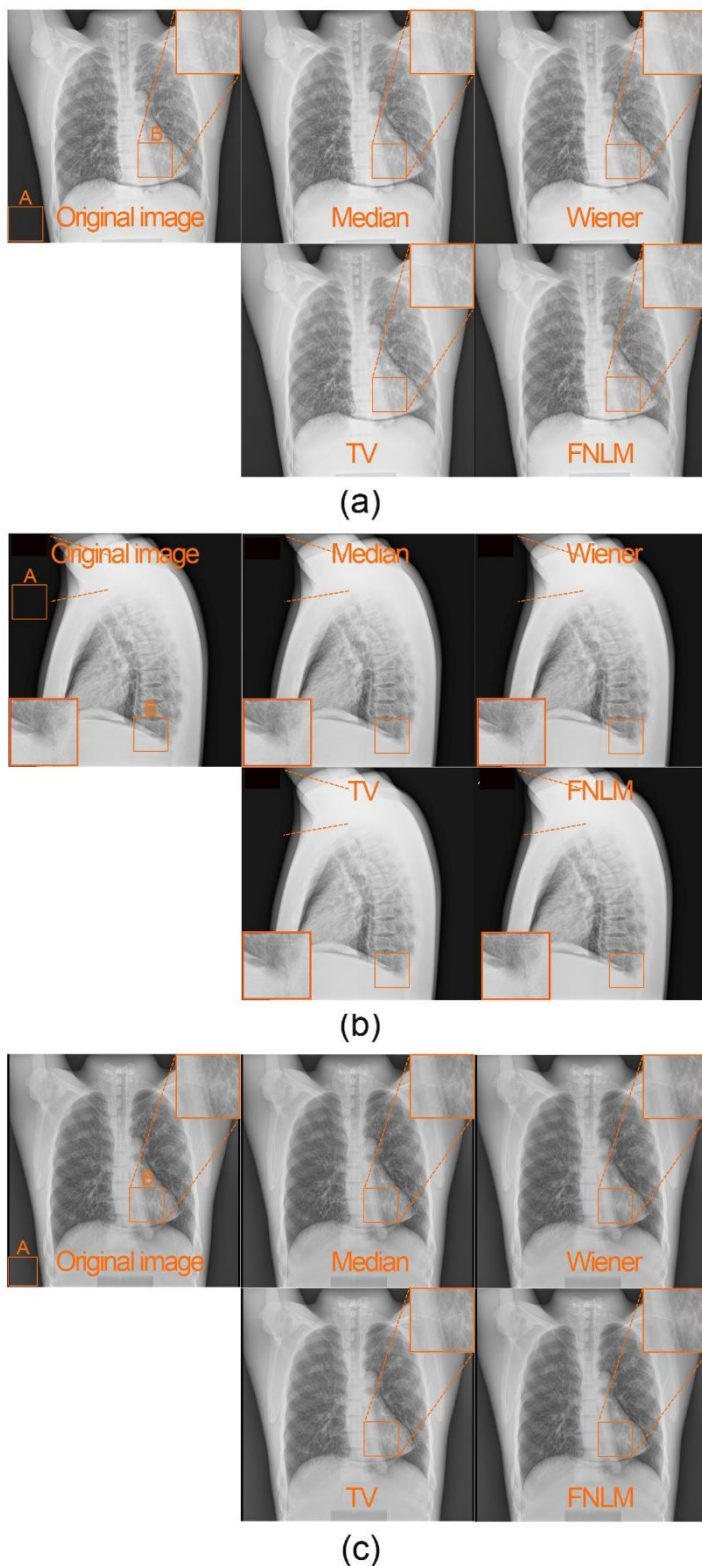


Figure 3. Chest phantom images with four applied filters, i.e., median, Wiener, TV, and FNLM, in the (a) AP, (b) LAT, and (c) PA positions. NNPS, COV, and CNR were obtained for the quantitative evaluation at ROIs A and B using images that depended on eight dose steps.

### Results

The NNPS evaluates the distribution of the overall noise. The corresponding values were highest (approximately  $10^{-3} \text{ mm}^2$ ) with the Wiener filter among

the filters in the AP, LAT, and PA positions, and lowest with the FNLM filter (approximately  $10^{-5} \text{ mm}^2$ ). In the AP, LAT, and PA positions, the image at 120 kVp and 1 mAs had the lowest NNPS value in the AP position, which was the smallest at 120 kVp and 30 mAs in the LAT

position, and 120 kVp and 5 mAs in the PA position. From the results, the higher the dose, the lower the NNPS that can be achieved. In the AP position, the NNPS value is the lowest when applying the FNLM filter, even though the radiation dose is the smallest at 120 kVp and 1 mAs.

At all positions, the highest COV value was obtained with the median filter, while the lowest was obtained with the FNLM filter. With the FNLM filter at the AP, LAT, and PA positions, the average COV values were 50%, 38%, and 15% lower than those of the original image. The COV values were analyzed for each position depending on the radiation dose. In the AP and PA positions, the image with 120 kVp and 1 mAs exhibited the lowest COV value, while in the LAT position, the lowest was at 120 kVp and 20 mAs. In the AP and PA images, most noises were removed using the FNLM filter in the image with the smallest dose.

From the CNR results, the median filter demonstrated the highest value at all positions, while the lowest value was realized with the FNLM filter. When using the FNLM filter at the AP, LAT, and PA positions, the CNR revealed noise reductions of 32%, 35.7%, and 18% on average from the original image. In the AP position, the image at 120 kVp and 5 mAs showed the highest CNR value; in the LAT position, the highest was at 120 kVp and 4 mAs, and in the PA position, it was the highest at 120 kVp and 1 mAs.

As shown in Fig. 4, the COV and CNR were measured at four locations where the nodules were located. In Fig. 4, a quantitative evaluation was performed by setting the ROI size to include the entire nodule in the chest image. Considering the COV, the FNLM filter exhibited the lowest value under all combinations of tube voltage and charge. Further, when using the FNLM filter, the noise was improved on average by 24% in ROIs 1, 2, and 3, and by 16% in ROI 4. In particular, the largest rates of decrease in the COV compared with the original image among all combinations of tube voltage and charge are at 120 kVp and 1 mAs in ROIs 1, 2 and 4, and at 120 kVp and 5 mAs in ROI 3, respectively (Fig. 5). The FNLM filter showed the highest CNR value under all combinations of tube voltage and charge, except in ROI 4. Here, the TV filter performed better. When using the FNLM filter in ROIs 1, 2 and 3, the CNR revealed average noise reductions of 13%, 12.5%, and 17% from the original image. In ROI 4, compared with the original image, the CNR improved by 9.5% when using the TV filter. In particular, the largest rates of increase in the CNR compared with the original image among all combinations of tube voltage and charge are at 120 kVp and 1 mAs in ROIs 1,2 and 3, and at 120 kVp and 4 mAs in ROI 4 (Fig. 6). The FNLM filter has a high CNR value and a low COV value, which significantly reduces image noise.

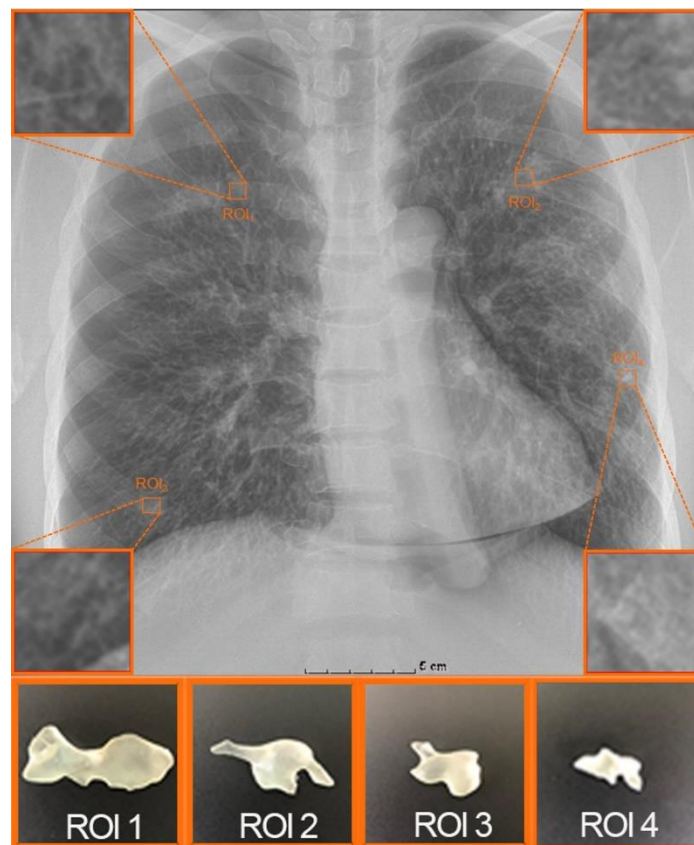


Figure 4. Chest phantom image in the AP radiography position where a nodule is located for a quantitative evaluation of the COV and CNR in ROIs 1, 2, 3, and 4, and background.

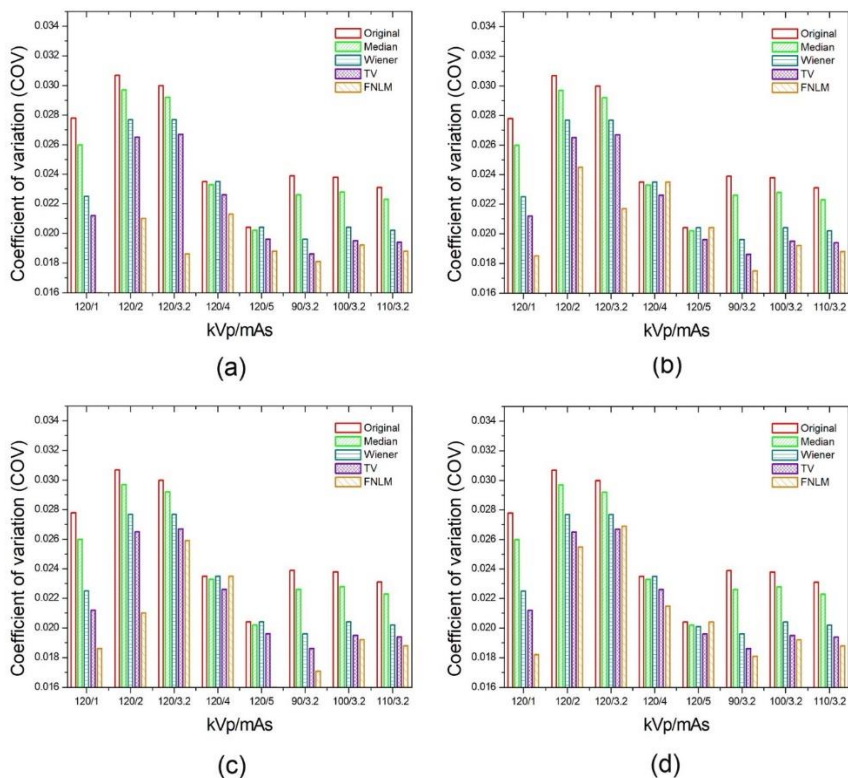


Figure 5. COV results in (a) ROI 1, (b) ROI 2, (c) ROI 3, and (d) ROI 4 for the median, Wiener, TV, and FNLM filters depending on radiation dose in the AP position.

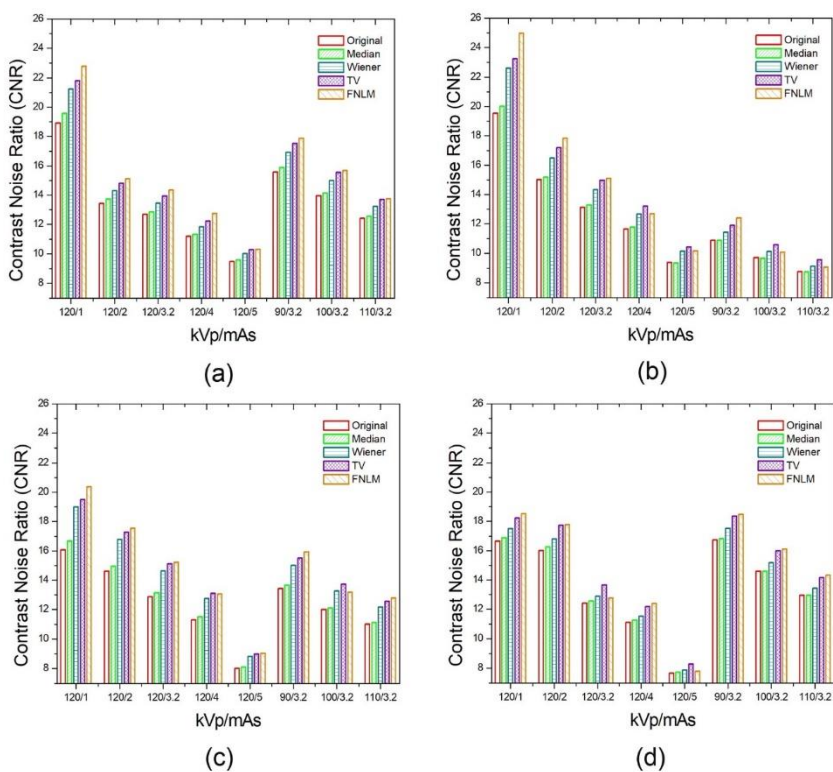


Figure 6. CNR results in (a) ROI 1, (b) ROI 2, (c) ROI 3, and (d) ROI 4 for the median, Wiener, TV, and FNLM filters depending on radiation dose in the AP position.

## Discussion

The lower the tube charge, the lower the radiation dose to a patient. However, a small number of photons cannot sufficiently penetrate a patient's body, resulting in excessive noise in the image. For example, in a CT image, artifacts are generated because photons do not sufficiently penetrate the shoulder portion, resulting in noise [23, 24]. A lower tube charge leads to degradation of image quality, owing to noise increase, but the use of an image filter allows removal of noise [9, 25, 26]. In addition, noise reduction using an image filter might reduce the signal difference caused by dose reduction. [27]. In another quantitative evaluation, decreasing the tube charge more than the tube voltage in the image has a strong effect on the image quality [28]. However, the use of a lower tube voltage can reduce patient doses more effectively than that of a low tube charge. A previous study has reported that tube voltage has a greater effect on patient doses [7]. Therefore, the use of the FNLM filter, after lowering tube voltage and raising tube charge, is recommended. First, lowering tube voltage significantly reduces the patient dose but degrades the image quality. To compensate for this, it is possible to supplement the image quality by raising the tube charge at the line that does not exceed the existing patient dose. The FNLM filter can then be used to maintain the image quality while lowering the patient's dose.

## Conclusion

In this study, the utility of fast non-local means (FNLM) filters to reduce radiation dose was investigated on images acquired from an adult chest phantom inserted with a nodule phantom fabricated via 3D printing based on a real patient's nodule shape. The experimental images were quantitatively evaluated by applying four filters (median, Wiener, TV and FNLM), in the AP, LAT, and PA positions while changing the tube voltage and radiation dose. The FNLM filter exhibited the best performance in the quantitative evaluation compared with the original image in all positions depending on the radiation dose. In addition, noise reduction using the FNLM filter was the most effective for images with high noise because it minimized the radiation dose required. For this reason, the use of FNLM filters to maintain diagnostic accuracy, while lowering the radiation dose, is beneficial for preventing cancer.

## References

- Schauer DA, Linton OW. NCRP report No. 160, ionizing radiation exposure of the population of the United States, medical exposure—are we doing less with more, and is there a role for health physicists? *Health Phys.* 2009;97(1):1-5.
- Do KH, Jung SE. Current status of medical radiation exposure in Korea—recent efforts to develop a radiation exposure control system focussed on justification and optimisation. *Annals of the ICRP.* 2016 Jun;45(1\_suppl):113-21
- Uffmann M, Schaefer-Prokop C. Digital radiography: the balance between image quality and required radiation dose. *European journal of radiology.* 2009 Nov 1;72(2):202-8.
- Geijer H, Norrman E, Persliden J. Optimizing the tube potential for lumbar spine radiography with a flat-panel digital detector. *The British Journal of Radiology.* 2009 Jan;82(973):62-8.
- Kim H, Park M, Park S, Jeong H, Kim J, Kim Y. Estimation of absorbed organ doses and effective dose based on body mass index in digital radiography. *Radiation protection dosimetry.* 2013 Jan 1;153(1):92-9.
- Hill KD, Einstein AJ. New approaches to reduce radiation exposure. *Trends in cardiovascular medicine.* 2016 Jan 1;26(1):55-65.
- Brenner DJ, Hall EJ. Computed tomography—an increasing source of radiation exposure. *New England journal of medicine.* 2007 Nov 29;357(22):2277-84.
- Kang H, Lee ES, Park HJ, Park BK, Park JY, Suh S-W. Abdominal digital radiography with a novel post-processing technique: phantom and patient studies. *Journal of the Korean Society of Radiology.* 2020 Jul 1;81(4)
- Anam C, Adi K, Sutanto H, Arifin Z, Budi WS, Fujibuchi T, Dougherty G. Noise reduction in CT images using a selective mean filter. *Journal of biomedical physics & engineering.* 2020 Oct;10(5):623.
- Lim JS. Two-dimensional signal and image processing. New Jersey: Englewood Cliffs; 1990.
- Strong D, Chan T. Edge-preserving and scale-dependent properties of total variation regularization. *Inverse problems.* 2003 Nov 12;19(6):S165.
- Buades A, Coll B, Morel J-M. A review of image denoising algorithms, with a new one. *Multiscale modeling & simulation.* 2005;4(2):490-530.
- Darbon J, Cunha A, Chan TF, Osher S, Jensen GJ. Fast nonlocal filtering applied to electron cryomicroscopy. *In 2008 5th IEEE International Symposium on biomedical imaging: from nano to macro 2008 May 14 (pp. 1331-1334).* IEEE.
- Doo K, Kang E, Yong H, Woo O, Lee K, Oh Y. Accuracy of lung nodule volumetry in low-dose CT with iterative reconstruction: an anthropomorphic thoracic phantom study. *The British Journal of Radiology.* 2014 Sep;87(1041):20130644.
- Buades A, Coll B, Morel J-M. A non-local algorithm for image denoising. *In 2005 IEEE Computer Society Conference on Computer Vision and Pattern Recognition (CVPR'05) 2005 Jun 20 (Vol. 2, pp. 60-65).* IEEE.
- Yaroslavsky LP. *Digital picture processing: an introduction.* Berlin: Springer Science & Business Media; 2012. Dec 6.
- Tomasi C, Manduchi R. Bilateral filtering for gray and color images. *In Sixth international conference on computer vision (IEEE Cat. No. 98CH36271) 1998 Jan 7 (pp. 839-846).* IEEE.
- Smith SM, Brady JM. SUSAN—a new approach to low level image processing. *International journal of computer vision.* 1997 May;23(1):45-78.
- Tschumperlé D, Brun L. Non-local image smoothing by applying anisotropic diffusion PDE's in the space

- of patches. In 2009 16th IEEE International Conference on Image Processing (ICIP) 2009 Nov 7 (pp. 2957-2960). IEEE.
20. Ghetti C, Borrini A, Ortenzia O, Rossi R, Ordóñez PL. Physical characteristics of GE Senographe Essential and DS digital mammography detectors. *Medical physics*. 2008 Feb;35(2):456-63.
  21. Brown CE. *Applied multivariate statistics in geohydrology and related sciences*. Berlin: Springer; 1998. p. 155-157.
  22. Varghese T, Ophir J. An analysis of elastographic contrast-to-noise ratio. *Ultrasound in medicine & biology*. 1998 Jul 1;24(6):915-24.
  23. Lee T-Y, Chhem RK. Impact of new technologies on dose reduction in CT. *European journal of radiology*. 2010 Oct 1;76(1):28-35..
  24. Hsieh J. Adaptive streak artifact reduction in computed tomography resulting from excessive x-ray photon noise. *Medical Physics*. 1998 Nov;25(11):2139-47..
  25. Shim J, Yoon M, Lee Y. Feasibility of newly designed fast non local means (FNLM)-based noise reduction filter for X-ray imaging: A simulation study. *Optik*. 2018 May 1;160:124-30.
  26. Konst B, Nøtthellen J, Naess SN, Båth M. Novel method to determine recursive filtration and noise reduction in fluoroscopic imaging – a comparison of four different vendors. *Journal of Applied Clinical Medical Physics*. 2021 Jan;22(1):281-92.
  27. Hatt CR, Oh AS, Obuchowski NA, Charbonnier J-P, Lynch DA, Humphries SM. Comparison of CT lung density measurements between standard full-dose and reduced-dose protocols. *Radiology: Cardiothoracic Imaging*. 2021 Apr;3(2).
  28. Wittenberg R, Peters JF, Sonnemans JJ, Bipat S, Prokop M, Schaefer-Prokop CM. Impact of image quality on the performance of computer-aided detection of pulmonary embolism. *American Journal of Roentgenology*. 2011;196(1):95-101.